Electric Breakdown in Liquids: Faster Ignition Using Less Energy

Ting-Ting Yan, Xiao-Xia Zhong,* Amanda E. Rider, Kostya (Ken) Ostrikov

The formation of vapor layers around an electrode immersed in a conducting liquid prior to generation of a plasma discharge is studied using numerical simulations. This study quantifies and explains the effects of the electrode geometry and applied voltage pulses, as well as the electrical and thermal properties of the liquids on the temporal dynamics of the pre-breakdown conditions in the vapor layer. This model agrees well with experimental data, in particular, the time needed to reach the electrical breakdown threshold. Because the time needed for discharge ignition can be accurately predicted from the model, the parameters such as the pulse shape, voltage, and electrode configuration can be optimized under different liquid conditions, which facilitates a faster and more energy-efficient plasma generation.

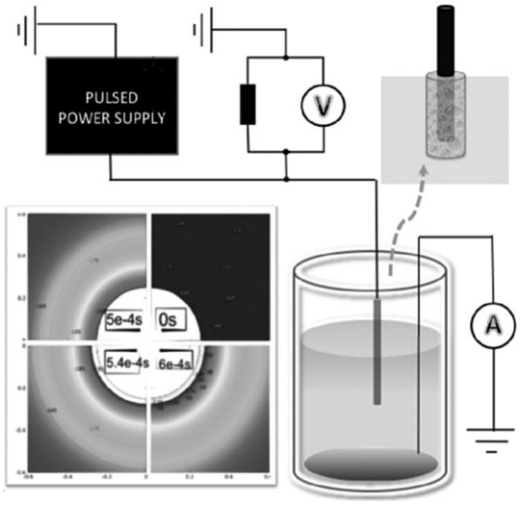

1. Introduction

Due to their environment-friendly nature and a host of highly reactive species,[1,3] plasmas produced by electrical discharges in liquids have been developed for a range of novel applications including pollution treatment,[4] water purification,[5] medical sterilization,[6,7] biological decontamination,[7] pathogen inactivation,[8] nanomaterials synthesis,[9] nanoscale assembly,[10,11] and plasma-based electrosurgical devices.[12,13] Various experimental conditions may be used to produce plasma discharges in the gas or liquid phase. Organic[14] or inorganic i.e., NaCl[12,13] liquids may be used, the power source voltage can range from 200 to 10 kV,[15,16] and the frequency can range from DC to GHz. A common feature in these processes is that a vapor layer and bubbles are observed before the plasma is generated.[17] It is generally accepted that, when the electric field within the vapor layer reaches $\sim 10^6\ \mathrm{V \cdot m^{-1}}$, it is high enough to cause the electrical breakdown and ignite a plasma.[2,3] For different solutions, properties such as electrical conductivity, thermal conductivity, heat capacity, and mass density are expected to have a different effect on the vapor layer formation process. Indeed, even for the same liquid, varying the electrode size and configuration and the applied voltage will influence the process of vapor layer formation; this relationship is presently poorly understood. Recently, the production of plasmas in saline solutions has been studied by varying solution boiling points at low voltages.[2,18] The parameters of the vapor layer were measured, and a reasonable agreement with numerical simulations was demonstrated. However, understanding and precisely describing the mechanism

T.-T. Yan, Prof. X.-X. Zhong
Key Laboratory for Laser Plasmas and Department of Physics, Shanghai Jiao Tong University, Shanghai 200240, People's Republic of China
E-mail: xxzhong@sjtu.edu.cn
A. E. Rider, K. Ostrikov
CSIRO Materials Science and Engineering, P. O. Box 218, Lindfield, NSW 2070, Australia
A. E. Rider, K. Ostrikov
Plasma Nanoscience @ Complex Systems, School of Physics, The University of Sydney, Sydney, NSW 2006, Australia

Plasma Process. Polym. **2013**, DOI: 10.1002/ppap.201200160

DOI: 10.1002/ppap.201200160

of the plasma formation in liquids still remain a challenge. Moreover, with the current emphasis on energy efficiency, it is important to be able to form the plasmas as quickly as possible and using the lowest possible amount of energy. This necessitates a thorough study of the effects of applied voltage (shape, amplitude, pulse, etc.), electrode size/configuration and liquid properties (e.g., electrical, thermal, electrochemical, etc.) to find the optimal configuration in terms of energy outlay. In order to have a better physical understanding of liquid discharge processes supported by various excitation schemes, this paper focuses on the temporal dynamics of the pre-breakdown conditions in the vapor layer. Indeed, the control of the temporal dynamics of pre-breakdown phenomena is very important in electrical insulation.[10,19] Despite the efforts of other authors,[10,19–22] pre-breakdown phenomena in liquids is an area that remains largely unexplored and requires further investigation. Here, we examine the relationship between the vapor layer growth over the electrode and adjustable parameters including the solution parameters, applied voltage, and electrode diameter. Hence, the simulation will assist with the choice of an appropriate pulse voltage for liquid discharges under different solution and energy supply parameters for faster and energy-efficient plasma generation.

The paper is organized as follows. The next section describes the model and computational method used. This is followed by the results and discussion section. In particular, the effect of electrical conductivity, specific heat, thermal capacity, applied voltage, current, electrode diameter, etc. on the vapor layer formation around the electrode are examined. Finally, conclusions and an outlook for future research are presented.

2. Model and Computational Method

Figure 1 is a schematic of the experimental setup considered in the simulation. A cylindrical tungsten negative electrode is inserted into a 0.9% NaCl solution see Table 1[23–27] for details, whereas the flat positive electrode is located at the bottom of the cuvette. A rectangular pulse is applied to the negative electrode with a pulse width that ensures discharge ignition will occur during the period simulated (i.e., the pulse duration is longer than the time needed for plasma ignition; hence the situation can be treated as a continuous DC power source during the 1 ms simulation time considered). Note, however, that the discharge ignition itself is not modeled in this paper. It will be shown that the shortest time needed to meet the conditions for ignition can be predicted by the simulation. As noted in the introduction, this is crucial for faster and energy-efficient discharge production.

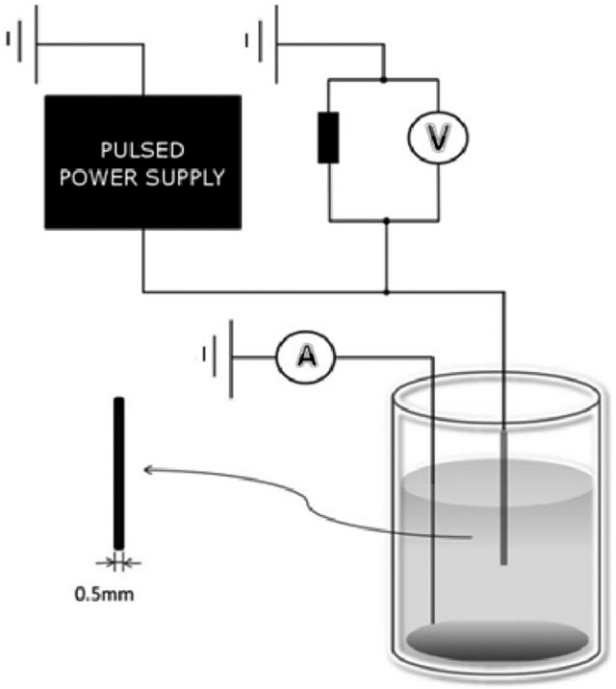

Figure 1. Schematic of the electrodes configuration and power supply used in simulations.

The growth of the vapor layer over the electrode was studied using COMSOL Multiphysics finite element modeling software.[28] An Ohmic-heating component, which

Table 1. The details of the standard 0.9% NaCl solution depending on the Equation (5)–(7), rounded to 2 significant digits; for full values please see ref.[2]

	σ (S · m^{-1})	ε	K (W · m^{-1} · K^{-1})	ρ (kg · m^{-3})	C (J · kg^{-1} · K^{-1})
c_0	2.8	2.8×10^{2}	-5.0×10^{-1}	2.8	4.4×10^{-4}
c_1	-3.9×10^{-2}	-1.0	6.0×10^{-3}	6.4	-5.1×10^{2}
c_2	1.2×10^{-4}	1.1×10^{-2}	-7.5×10^{-6}	-1.8×10^{-2}	2.3
c_3				1.5×10^{-5}	-4.6×10^{-3}
c_4					3.4×10^{-6}
P_V	3.2×10^{-10}	1.0	2.5×10^{-2}	6.0×10^{-1}	2.0

coupled the heat transfer component with a generalized electrostatics module, was developed.[18] The electric field was found using the following Equation (1)–(3):[16]

$$\vec{J} = \sigma(T)\cdot\vec{E} \tag{1}$$

$$\nabla\cdot(\varepsilon(T)\cdot\vec{E}) = 0 \tag{2}$$

$$\vec{E} = -\nabla V \tag{3}$$

where $\vec{J}$ is the current density, $\sigma(T)$ is the electrical conductivity, T is the temperature, $\vec{E}$ is the electric field, $\varepsilon(T)$ is the dielectric constant and V is the electric potential. The thermal properties are described by the time-dependent heat conduction Equation (4):[18]

$$\rho(T)C_{\mathrm{p}}(T)\frac{\partial T}{\partial t} - \nabla\cdot(K(T)\nabla T) = \vec{J}\cdot\vec{E} \tag{4}$$

where $\rho(T)$ is the mass density, $C_{\mathrm{p}}(T)$ is the specific heat, t is the time, $K(T)$ is the thermal conductivity and $\vec{J}\cdot\vec{E}$ is the Ohmic-heating term covering the whole liquid region.

Simulating the vapor formation process is simplified by the use of Heaviside step functions, H, to describe model parameters, ignoring the latent heat of vaporization and the phase change as follows:

$$P(T) = P_{\mathrm{L}}[1 - H(T - T_{\mathrm{vap}})] + P_{\mathrm{V}}H(T - T_{\mathrm{vap}}) \tag{5}$$

$$P_L(T) = c_0 + c_1T + c_2T^2 + c_3T^3 + c_4T^4 \tag{6}$$

$$P_{\mathrm{V}} = \mathrm{const} \tag{7}$$

where $P(T)$ is a parameter which represents electrical conductivity, $\sigma(T)$, relative permittivity $\varepsilon(T)$, thermal conductivity $K(T)$, mass density $\rho(T)$ or specific heat $C(T)$ of the liquids and vapors studied. The parameter $P_{\mathrm{L}}(T)$ refers to properties in the liquid phase that are a function of the temperature, P_{V} refers to the property in the vapor phase that is assumed to be constant in the model and T_{vap} is the vaporization temperature, c_0–c_4 are coefficients defined in Table 1.

To save computation time, a 1D-axisymmetric model was chosen to simulate the vapor layer growth dependent on the applied voltage, electrode diameter and solution properties. The problem was solved using a transient solver, with the calculated results recorded at various intervals. A 0.9% NaCl solution at room temperature (293.15 K) was selected as the standard solution. However, since various applications use various solution discharges (from water treatment to nanomaterial fabrication) and involve liquids whose electrical conductivity, heat capacity and mass density values vary over several orders of magnitude,[3] a series of test solutions was also studied. In these studies, scale coefficient *kk* was used to represent the ratio of the electric conductivity, the heat capacity and the mass density of the test solution relative to that of the standard solution. Results were then plotted to establish the dependence of the vapor layer formation around the electrode on solution heat and electrical conductivity, solution mass density, applied voltage, electrode diameter, etc.

3. Results and Discussion

Here, we present two-dimensional temperature and electric potential distributions based on the standard solution, followed by the effect of varied applied voltage, electrode diameter and solution parameters on temporal evolution of: the electric field, the current density, and the energy flux density.

3.1. 2D Temperature and Potential Distribution

Figure 2 shows the time and spatial evolution of the temperature and the potential distribution around the electrode in solution after the pulsed voltage is applied to the electrode. The model geometry is 1D axisymmetric, the cross-section figure is plotted containing only one quadrant perpendicular to the water surface. The color represents the temperature: red regions are hotter than blue regions, whereas the contour lines represent the electric potential.

Figure 2a shows the initial state for the liquid around the electrode, before a vapor is formed. The potential contour plot shows that the closer the region is to the electrode, the higher the electric field gets. Figure 2b represents the situation 0.5 ms later; here, the temperature of the solution increases, but is still lower than the boiling point, hence the vapor has not formed. As seen from Figure 2c, at 5.6 ms, vapor has formed. However, since (1) not enough vapor has formed and (2) the potential is still distributed through the whole liquid – not concentrated as required, a discharge will not ignite under these conditions. After 6 ms into the process, enough vapor was formed and the electric field was strongly concentrated in the vapor layer, shown in Figure 2d. Thus, it is clear that the vapor layer over the electric field serves as a good dielectric material in which the electric field is high enough for a discharge to ignite.

As in ref.[18], the equipotential lines tend to concentrate in the low-conductivity regions (i.e., the water vapor in the vapor layer) and the electric field there is enhanced. As noted, when the electric field strength within the vapor layer reaches about $10^6\,\mathrm{V\cdot m^{-1}}$, this value is high enough to cause an electrical breakdown between the vapor layer and the electrode, which ignites the plasma right away. This vapor layer remains 50 μm thick, as it spreads over the electrode and there forms the breakdown electric field. Our

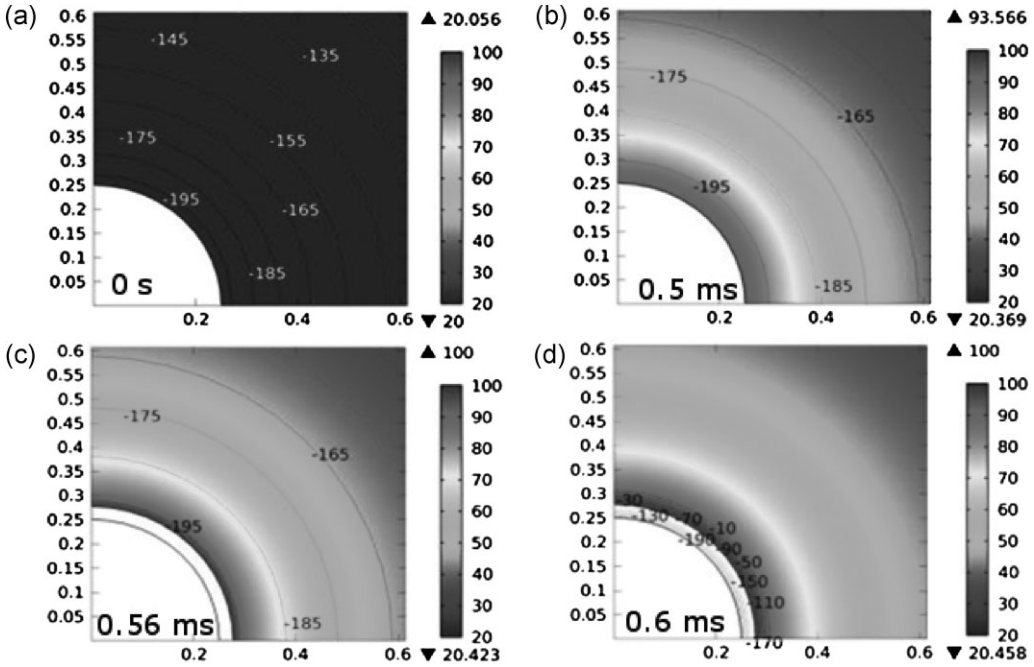

Figure 2. 2D surface temperature plots (color scale at right); contour plots for electric potential shows vapor layer production and the model results obtained at −200 V. (a) initial time (white color refers to the electrode part which is not computed); (b) 0.5 ms; (c) 0.56 ms (new white region indicates vapor for temperatures above 100 °C; (d) 0.6 ms (electric potential concentrated on the vapor layer).

simulated thickness for the vapor layer was smaller than the experimental result.[2] A possible reason is that there is some air dissolved in the liquid. Before the liquid is vaporized by Ohmic heat, air evaporates from the liquid in the experiment, and this contribution to the vapor is not considered in our model. As a result, the vapor layer in the experiment may be thicker. Likewise, our results show that the location of initial vaporization in the experiment is near the flat part of the electrode rather than near the sharp rim as reported in ref.[2], which may be also caused by the remaining gas in the solution. Further experiments and simulations are required to confirm this possibility.

3.2. The Temporal Evolution of the Electric Field

Here, the effect of the voltage and electrode diameter, as well as of some solution properties (electrical conductivity, heat capacity and mass density) on the temporal evolution of the electric field are studied.

3.2.1. The Effect of Applied Voltage and Electrode Diameter

Figure 3a illustrates the temporal evolution of the electric field from the rim of the tungsten electrode with applied voltages ranging from 200 to 800 V. The electric field increases rapidly as soon as the vapor layer is formed. It takes 0.6 ms for the electric field strength to reach $10^7\ V \cdot m^{-1}$ when the applied pulse voltage is 200 V and the electrode diameter is 0.5 mm. This result is in a good agreement with the experimental findings,[16] where 0.6 ms is the shortest time needed for a solution discharge to ignite at a voltage of 200 V and electrode diameter of 0.5 mm. In the experiments, vapor formation, plasma formation, vapor collapse, and subsequent pressure wave propagation were observed.[2,18] For different voltages, the temporal evolution of the electric field was similar. Higher voltages led to a faster and larger increasing electric field. From Figure 3a, it can be seen that the tendency presented in our plots is consistent with experimental results.[2,18]

The temporal evolution of the electric field with electrode diameter is shown in Figure 3b. By decreasing the diameter of the negative electrode from 0.6 to 0.4 mm, the time required for the formation of the peak electric field also decreases, whilst the peak electric field magnitude remains constant. This result is reasonable, as the narrow electrode simply accelerates the vapor formation over the electrode, but does not change the spatial structure of the vapor layer. Obviously, a smaller diameter of the electrode means that a lower pulsed voltage can be used to achieve plasma ignition when compared to thicker electrodes and higher pulsed voltages. This observation is very important from an energy efficiency point of view.

3.2.2. The Effect of the Liquid Properties

Figure 4a plots the temporal evolution of the electric field for different electrical conductivities. It can be seen that the electric field breakdown values are not affected by the variation of the electrical conductivity of the test solution.

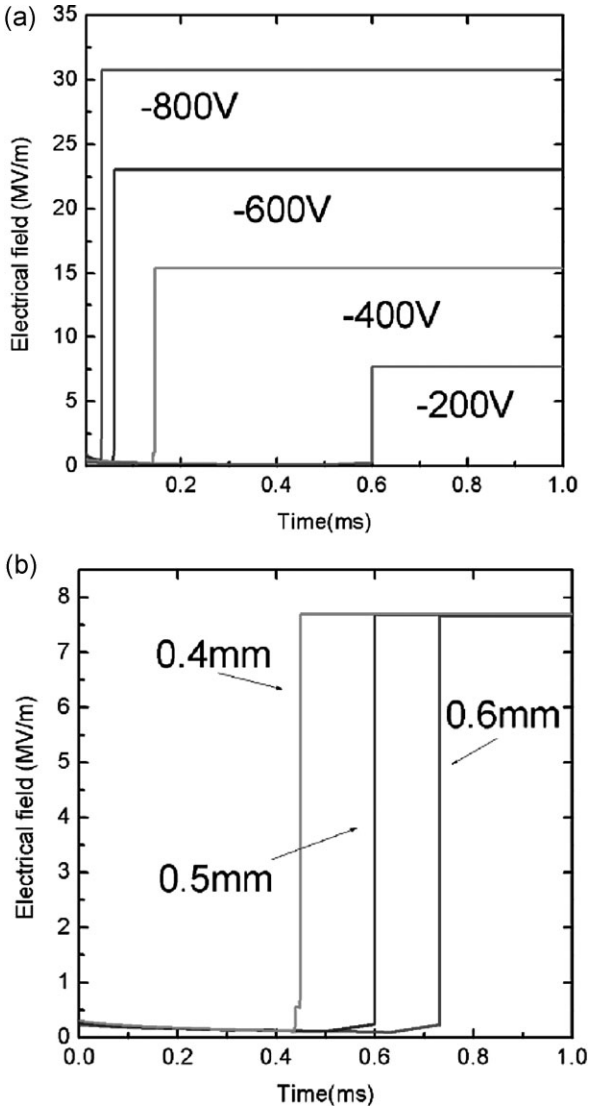

Figure 3. The computed time of the electric field in the vapor layer near the electrode under different parameters: (a) voltage of −200, −400, −600, and −800 V; (b) electrode diameter of 0.6, 0.5, and 0.4 mm.

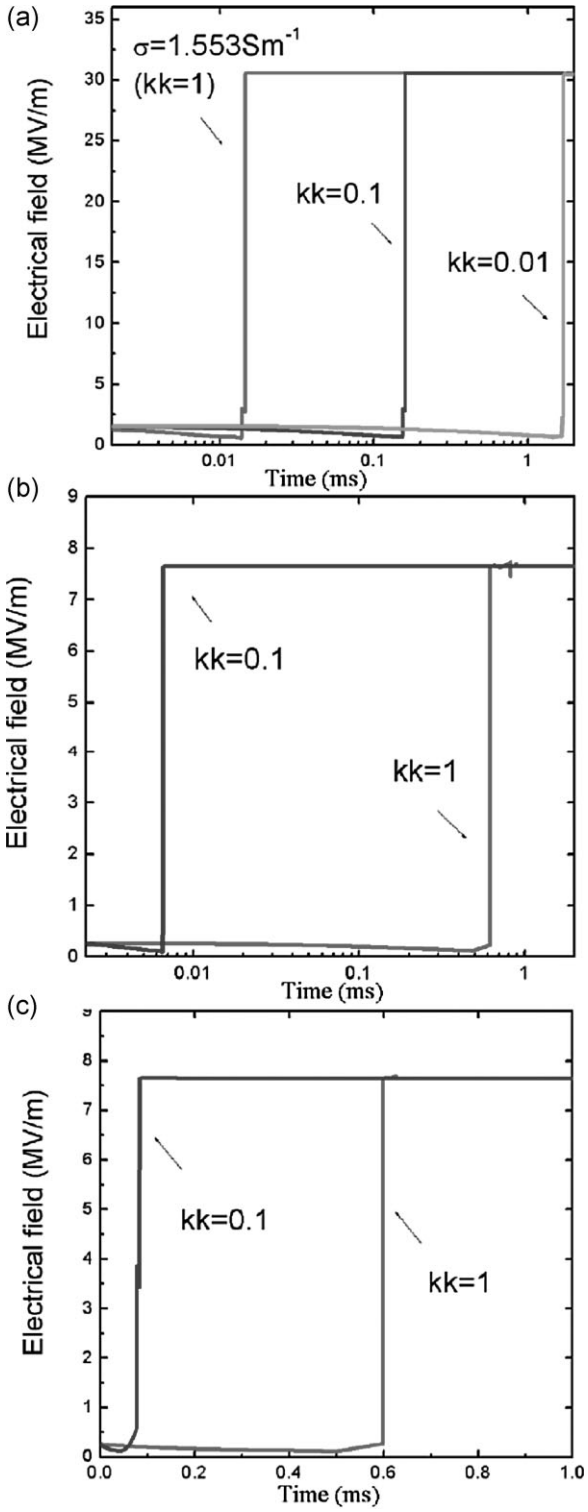

Figure 4. The computed electric field histories near the electrode for various liquid parameters: (a) electrical conductivity at −800 V; (b) heat conductivity at −200 V; (c) mass density at −200 V.

However, increasing the electric conductivity by two orders of magnitude leads to a decrease in the time needed to form the vapor over the electrode by two orders of magnitude. Since the electrical conductivity of the solution has no influence on the thickness of the vapor layer, it is reasonable to believe that the electric field breakdown value is unchanged at different electrical conductivities. According to the Ohmic heating law, when the electrical conductivity is lower, so is the efficiency of the transformation of electrical energy into thermal energy. In other words, it takes a longer time to develop a vapor layer over the electrode and induce a sufficiently strong electric field for discharge ignition by decreasing the electrical conductivity

of the solution, see Figure 4a. Figure 4b and c show the dependence of the temporal evolution of the electric field on the liquid heat capacity and mass density. When the heat conductivity or mass density of the liquid is decreased by one order of magnitude, one order of magnitude shorter time is needed for the vapor and the high electric field to form over the electrode surface. Here, a shorter time for vapor layer growth over the electrode surface is obtained by decreasing the specific heat and the mass density of solution. The result can be explained as follows: by decreasing the specific heat or the mass density of the solution, less energy per unit volume is needed to transform the liquid into vapor; as a result, the vapor layer over the electrode forms faster. Hence, the plasma may be generated using less energy if a solution with lower specific heat and mass density is used.

3.3. The Temporal Evolution of the Current Density

With the vapor layer growing over the electrode, the temporal evolution of the current density is plotted in Figure 5. Comparing Figure 5a and b, it can be noticed that the initial current density is a function of the applied voltage, but is independent of the mass density. In both Figure 5a and b, there is a turning point in the temporal evolution curve of the current density. Indeed, the current density increases with time until arriving at this point whereupon it decreases rapidly. The results mentioned above are reasonable according to Ohm's law. It is well known that the current density is the product of the electric field and conductivity of the solution. This is why the initial current density varies with the applied voltage and remains unchanged with the mass density. Depending on the behavior of the initial current density, the applied voltage, electrode diameter and the solution properties can be classified into two types, namely type I (affects peak value) and type II (does not affect peak value) parameters. Figure 5a represents the current dependence on a type I parameter. Here, the initial current density is shown to be a function of applied voltage – i.e., by decreasing the applied voltage, the initial current density decreases. Figure 5b represents the current dependence on type II parameters. Here, the initial current density does not depend on the solution properties - when the specific heat of the solution was increased or decreased, the initial current density remained unchanged. It can be expected that the electric conductivity and electrode diameter will be type I parameters, and that the mass density of solution will be a type II parameter. Since the current density is the product of the electric field and the conductivity of the solution, where the conductivity of the solution is a function of the temperature of the solution and increases with rising temperature, Ohmic heating causes the temperature of the solution to increase as shown in Figure 2b, and, as a result,

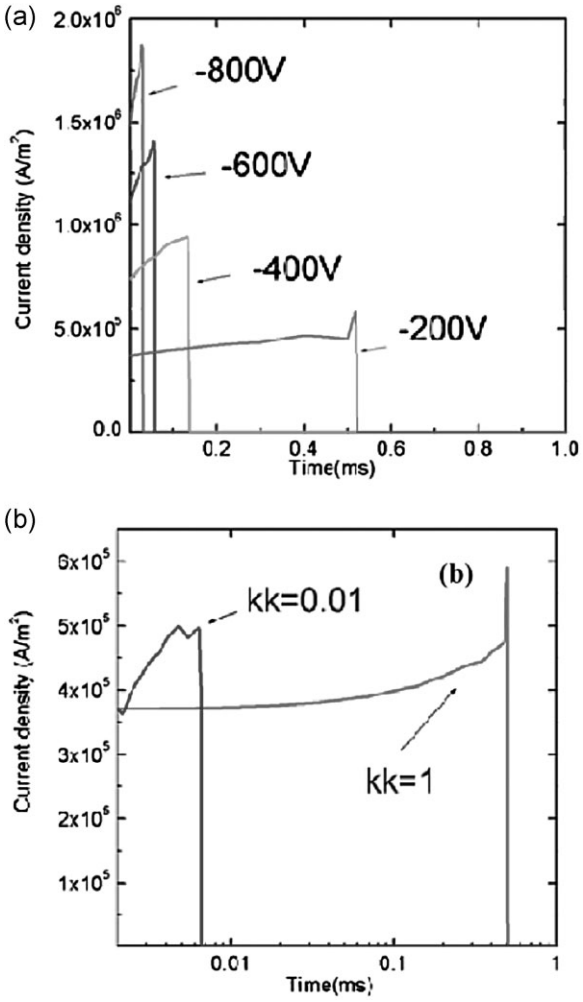

Figure 5. The computed temporal evolution of the current density in the vapor layer near the electrode under different parameters: (a) voltage; (b) heat conductivity.

the current density increases as seen in Figure 5a and b until the liquid is heated to the boiling point when the phase change from liquid to vapor takes place. As the solution is heated to the boiling point, the current density decreases abruptly due to the sudden decrease of the conductivity of the solution, so there is a turning point in the curve of the current density. This turning point in the current density reflects the time the phase change takes place. As it can be seen from the graph, this turning point occurs earlier due to higher voltages as the vapor is formed quicker. The tendency of the temporal evolution of the current density agrees well with the experimental result and the turning point of the current density almost coincides with the measured experimental value.[2] This agreement illustrates that the computed results are reasonable. By comparing Figure 3a and 5a, one can see that the behavior of the current density and the electric field are consistent with each other.

Interestingly, compared with the electric field, the current density responds earlier with the formation of vapor at the lower applied voltage of −200 V, and it tends to respond at the same time where electric field responds. It can be seen that the current density is more sensitive to the vapor formation than the electric field. Increasing the applied voltage, the vapor forms quickly, the difference between the responding time of the current density and the electric field with the vapor formation becomes too small to be discerned.

3.4. The Temporal Evolution of the Energy Flux Density

Figure 6a quantifies the temporal variation of the energy flux density under different electrical conductivity conditions, representative of type I behavior. Figure 6b shows the temporal evolution of the energy flux density at different mass densities, representative of type II behavior. As can be seen in Figure 6a, the higher the energy flux density, the faster the vapor is formed. The voltage and the liquid electrical conductivity, the type I parameters classified above, affect the energy flux density, as well as the time needed for the vapor layer to grow over the electrode. Although the energy flux density is different under varied applied voltages and solution electrical conductivities, the total energy needed for a vapor layer to form over the electrode remains unchanged. While the type II parameters, such as the liquid heat capacity and mass density, do not affect energy flux density, they affect the formation time of the vapor layer. The energy consumed for vapor layer formation is a function of the specific heat and the mass density of the solution. Therefore, less energy consumption for the plasma ignition can be expected for solutions with lower specific heat and mass density.

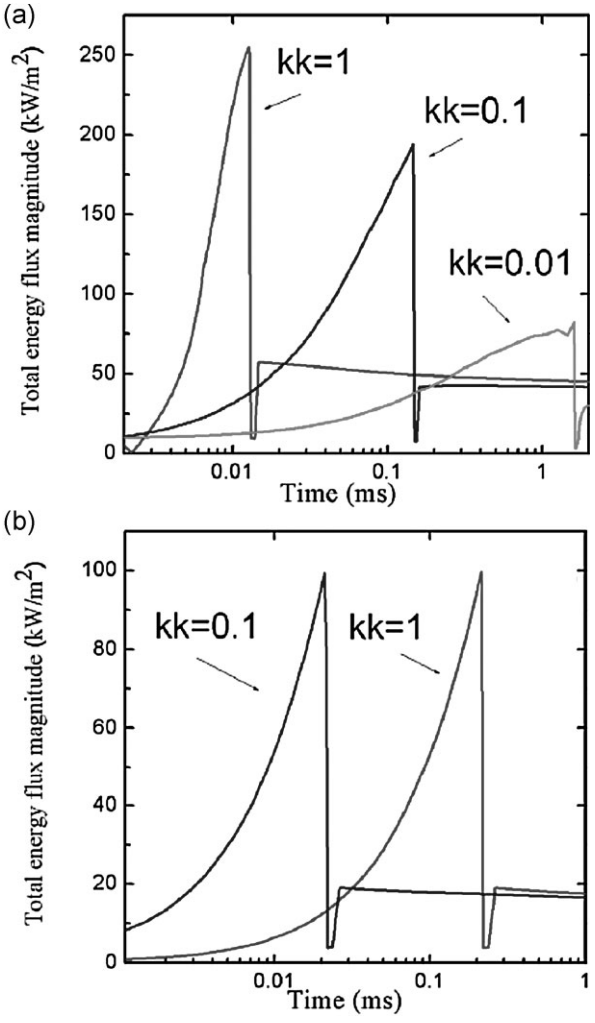

Figure 6. The computed temporal evolution of the energy flux density in the vapor layer near the electrode under different parameters: (a) electrical conductivity; (b) mass density.

3.5. Summary of the Simulation Results

To summarize, the effects of the applied voltage and electrode diameter are as follows:

(i) As the applied voltage is increased, the electric field becomes stronger and reaches the breakdown threshold faster. Similarly, the current density peaks faster and at a higher value of the applied voltage.
(ii) As the diameter of the negative electrode decreases, the peak electric field strength is reached quicker, whereas the electric breakdown value is constant.

The effect of the solution parameters is as follows:

(i) As the electrical conductivity of the solution increases, the vapor and subsequent plasma form faster, whereas the electric breakdown value remains unchanged. The energy flux density peaks faster and at a higher value of the electrical conductivity.
(ii) As the heat conductivity of the solution decreases, the peak electric field strength is reached quicker, whereas the electric breakdown value remains constant. Similarly, the current density peaks faster.
(iii) As the mass density of the solution decreases, the peak electric field strength is reached quicker, whereas the electric breakdown value remains constant. Moreover, the total energy flux magnitude peaks faster (but remains at the same value), for lower mass density of solution.

4. Conclusion

The dependence of the formation of the vapor layer and the dynamics of pre-breakdown phenomena in a plasma-liquid system on a wide range of parameters has been investigated numerically. As energy efficiency is a timely issue, particular emphasis was placed on finding the optimum combinations of the applied voltage, electrode diameter and solution parameters to ensure that the electrode would be covered by the vapor in as short a time as possible and using the lowest possible amount of energy. It was found that less energy will be consumed for vapor formation (and later, once the electric field reaches $\sim 10^6\,\mathrm{V}\cdot\mathrm{m}^{-1}$, the plasma ignition) if solutions with lower specific heat and mass densities are used. Moreover, if a thinner electrode is used, a lower pulsed voltage may ignite the plasma in a comparable time to a higher pulsed voltage and a thicker electrode. These conclusions are generic and will help improving energy efficiency of multipurpose solution plasma discharges. Future research should focus on examining similar effects in more application specific contexts, for example, optimizing discharges in ionic liquids for the purpose of nanoscale self-assembly.[29]

Acknowledgements: X.X.Z. and T.T.Y. acknowledge support from the *NSFC* (grant no. 90923005, 11275127), *STCSM* (grant no. 09ZR1414600), and the *National ITER Plans Program of China* (grant no. 2009GB105000). A.E.R. acknowledges the *CSIRO OCE Postdoctoral Fellowship & SSN-TCP* schemes. This work was partially supported by the *Australian Research Council* and *CSIRO OCE* Science Leadership Scheme.

Received: November 19, 2012; Revised: January 7, 2013; Accepted: January 18, 2013; DOI: 10.1002/ppap.201200160

Keywords: liquid plasmas; modeling; pulsed discharges; thermodynamics

[1] P. Lukes, B. R. Locke, J. L. Brisset, "Aqueos-Phase Chemistry of Electrical Discharge Plasma in Water and in Gas–Liquid Environments", in: *Plasma Chemistry and Catalysis in Gases and Liquids*, V. L. Parvulescu, M. Magureanu, P. Lukes, Eds., Wiley-VCH Verlag GmbH & Co. KgaA, Weinheim, Germany **2012**.

[2] L. Schaper, K. R. Stalder, W. G. Graham, *Plasma Sources Sci. Technol.* **2011**, *20*, 034004.

[3] W. G. Graham, K. R. Stalder, *J. Phys. D: Appl. Phys.* **2010**, *44*, 174037.

[4] Z. Yan, L. Chen, H. Wang, *J. Phys. D: Appl. Phys.* **2008**, *41*, 155205.

[5] J. Foster, B. S. Sommers, S. N. Gucker, I. M. Blankson, G. Adamovsky, *IEEE Trans. Plasma Sci.* **2012**, *40*, 1311.

[6] C. M. Du, J. Wang, L. Zhang, H. X. Li, H. Liu, Y. Xiong, *New J. Phys.* **2012**, *14*, 013010.

[7] A. Abou-Ghazala, S. Katsuki, K. H. Schoenbach, F. C. Dobbs, F. C. Dobbs, K. R. Moreira, *IEEE Trans. Plasma Sci.* **2002**, *30*, 1449.

[8] T. Maisch, T. Shimizu, Y. F. Li, J. Heinlin, S. Karrer, G. Morfill, J. L. Zimmermann, *PloS ONE* **2010**, *6*, e24104.

[9] D. Mariotti, R. M. Sankaran, *J. Phys. D: Appl. Phys.* **2010**, *43*, 323001.

[10] B. R. Locke, S. M. Thagard, *Plasma Chem. Plasma Process.* **2012**, *32*, 875.

[11] W. Yan, Z. J. Han, B. T. Phung, K. Ostrikov, *ACS Appl. Mater. Interfaces* **2012**, *4*, 2637.

[12] J. C. Jung, I. G. Koo, M. Y. Choi, Z. Yu, M. S. Kim, G. J. Collins, *Plasma Process. Polym.* **2012**, *9*, 463.

[13] L. Schaper, C. P. Kelsey, P. Ceccato, A. Rousseau, K. R. Stalder, W. G. Graham, *IEEE Trans. Plasma Sci.* **2011**, *39*, 2670.

[14] S. M. Thagard, K. Takashima, A. Mizuno, *Plasma Process. Polym.* **2009**, *6*, 741.

[15] P. Ceccato, O. Guaitella, L. Schaper, W. Graham, A. Rousseau, *IEEE Pulsed Power Conf. Process* **2009**, *2*, 863.

[16] P. H. Ceccato, O. Guaitell, M. R. L. Gloahec, A. Rousseau, *J. Phys. D: Appl. Phys.* **2010**, *43*, 175202.

[17] K. Y. Shih, B. R. Locke, *Plasma Process. Polym.* **2009**, *6*, 729.

[18] L. Schaper, W. G. Graham, K. R. Stalder, *Plasma Sources Sci. Technol.* **2011**, *20*, 034003.

[19] I. V. Timoshkin, M. J. Given, M. P. Wilson, R. A. Fouracre, S. J. Macgregor, Electrical Insulation and Dielectric Phenomena (CEIDP), 2010 Annual Report Conference on 2010, 1.

[20] R. P. Joshi, J. F. Kolb, S. Xiao, K. H. Schoenbach, *Plasma Process. Polym.* **2009**, *6*, 763.

[21] K. H. Schoenbach, J. Kolb, S. Xiao, S. Katsuki, Y. Minamitani, R. Joshi, *Plasma Sources Sci. Technol.* **2008**, *17*, 024010.

[22] M. Simek, M. Clupek, V. Babicky, P. Lukes, P. Sunka, *Plasma Sources Sci. Technol.* **2012**, *21*, 055031.

[23] A. Stogryn, *IEEE T. Microw. Theory* **1971**, *19*, 733.

[24] E. Colin, W. Clarke, D. N. Glew, *J. Phys. Chem. Ref. Data* **1985**, *14*, 489.

[25] M. Laliberté, W. E. Cooper, *J. Chem. Eng. Data* **2004**, *49*, 1141.

[26] H. Ozbek, S. L. Phillips, *J. Chem. Eng. Data* **1980**, *25*, 263.

[27] J. V. Sengers, J. T. R. Watson, *J. Phys. Chem. Ref. Data* **1984**, *13*, 893.

[28] COMSOL Multiphysics 2010 Version 4.0.

[29] T. L. Greaves, C. J. Drummond, *Chem. Soc. Rev.* **2008**, *37*, 1709.